Journal of Power Sources 196 (2011) 8207–8215

Contents lists available at ScienceDirect

Journal of Power Sources

journal homepage: www.elsevier.com/locate/jpowsour

Effects of anatase TiO_2 with different particle sizes and contents on the stability of supported Pt catalysts

Zheng-Zhi Jiang[a,b], Da-Ming Gu[b,**], Zhen-Bo Wang[a,c,*], Wei-Li Qu[a,b], Ge-Ping Yin[a], Ke-Jian Qian[c]

[a] School of Chemical Engineering and Technology, Harbin Institute of Technology, No. 92 West-Da Zhi Street, Harbin 150001, China
[b] School of Science, Harbin Institute of Technology, No. 92 West-Da Zhi Street, Harbin 150001, China
[c] Zhejiang Province Green Electric Power Products Quality Inspection Center, Economic Development Zone Located in Science and Technology Venture Park, Changxing 313100, China

ARTICLE INFO

Article history:
Received 17 March 2011
Received in revised form 23 May 2011
Accepted 24 May 2011
Available online 31 May 2011

Keywords:
Proton exchange membrane fuel cell
Mixed support
Titanium dioxide particle size
Titanium dioxide content

ABSTRACT

Pt/TiO_2–C catalyst with TiO_2 and carbon black as the mixed support has been synthesized by the microwave-assisted polyol process (MAPP). Effects of anatase TiO_2 with different particle sizes and contents on the stability of supported Pt catalysts have been systematically studied. X-ray diffraction (XRD), transmission electron microscopy (TEM), cyclic voltammograms (CV), and accelerated potential cycling tests (APCT) have been carried out to present the influence degree. The experimental results indicate that the original electrochemically active specific surface areas (*ESA*) of the catalysts decrease with the increase of mean particle sizes of TiO_2 and TiO_2 contents. However, the activity of Pt/TiO_2–C-20 is very close to that of Pt/TiO_2–C-5 and the stability of Pt/TiO_2–C-20 is the best after 1000 cycles APCT, illustrating that the optimized particle size of TiO_2 in Pt/TiO_2–C catalyst is 20 nm. Furthermore, the stability of the catalysts increase with the increase of TiO_2 contents in the mixed support. Taking into account both the activity and stability of various Pt/TiO_2–C catalysts, the optimized particle size of TiO_2 is 20 nm and the optimal TiO_2 content existed in the mixed support is 40%.

1. Introduction

Proton exchange membrane fuel cells (PEMFCs) have attracted increasing interest in recent years due to their high efficiency, high energy density, low-temperature operation, fast start-up, environmental friendliness and the possibility for a variety of applications [1–4]. Carbon black is still the most widely used catalyst support for PEMFCs as it has very high surface area, moderate pore structure, and excellent electronic conductivity [1,5–7]. However, carbon materials are susceptible to corrosion in PEMFCs [8–11], because they are exposed to an aggressive combination of strong oxidizing conditions, liquid water, strongly acidic conditions, high temperatures, high electrochemical potentials, high electric currents, and large potential gradients and so on [10–12].

More stable and corrosion-resistant catalyst supports are currently required in order to inhibit the corrosion of carbon support and increase the stability of the catalysts during the operation of PEMFCs. Recently, excellent mechanical resistance and stability of TiO_2 in acidic and oxidative environments make it popular in the PEMFCs catalyst field [13–15]. To date, the hydrolysis of titanium alkoxides is the main method by which TiO_2 was incorporated into the PEMFCs catalyst. Nevertheless, the catalysts synthesized through this method need to be heat-treated at high temperatures so that the mean particle size of Pt nanoparticles would increase. Xiong and his co-workers [16] prepared Pt/TiO_x/C nanocomposites for oxygen reduction in direct methanol fuel cells by three different routes and found that Pt/TiO_x/C nanocomposites exhibited better methanol tolerance than Pt/C. Pt/TiO_2/C synthesized with a two-step reaction method by Liu and his co-workers [17] was employed as cathode catalyst for PEMFC. After the same accelerated aging test (AAT), the mean particle size of the Pt in Pt/C increased from 5.3 to 26.5 nm in comparison with that in Pt/TiO_2/C increased from 7.3 to 9.2 nm, which indicated that Pt/TiO_2/C catalyst is more stable than Pt/C. In our previous work [18], we have reported that the microwave-assisted polyol process (MAPP) is a more rapid, simple, uniform, and efficient method to prepare Pt/TiO_2–C catalyst with TiO_2 and carbon black as the mixed support. Moreover, the Pt/TiO_2–C catalyst synthesized by this method exhibited both high activity and stability in comparison with Pt/C prepared by the same process. However, so far, the effects of anatase TiO_2 with different particle sizes and contents on the stability of Pt-based catalysts prepared by the MAPP have not been studied systematically yet, which is worth studying. In this paper, X-ray diffraction (XRD), transmission electron microscopy (TEM), cyclic voltammograms (CV), and accelerated potential cycling tests (APCT) for Pt/TiO_2–C catalysts

* Corresponding author at: School of Chemical Engineering and Technology, Harbin Institute of Technology, No. 92 West-Da Zhi Street, Harbin 150001, China. Tel.: +86 451 86417853; fax: +86 451 86418616.
** Co-corresponding author.
E-mail addresses: gudaming@126.com (D.-M. Gu), wangzhenbo1008@yahoo.com.cn (Z.-B. Wang).

0378-7753/$ – see front matter © 2011 Elsevier B.V. All rights reserved.
doi:10.1016/j.jpowsour.2011.05.063

have been carried out to present the influence degree of different particle sizes and contents of TiO_2.

2. Experimental

2.1. Catalyst preparation

Hexachloroplatinic acid ($H_2PtCl_6{\cdot}6H_2O$) was purchased from Shanghai, China. Vulcan XC-72 carbon black with mean particle size of 20 nm was purchased from E-TEK and 5 wt.% Nafion solution was obtained from Dupont. Anatase titanium dioxide (TiO_2) with particle sizes of 5, 20, 30, 50, and 70 nm was obtained from Xuan Cheng Jing Rui New materials Co., Ltd., China. Except where specified, all chemicals were of analytical grade and used as received. Pt/TiO_2–C catalysts with different particle sizes and contents of TiO_2 were synthesized by the microwave-assisted polyol process (MAPP) [18]. The total Pt metal loading was fixed

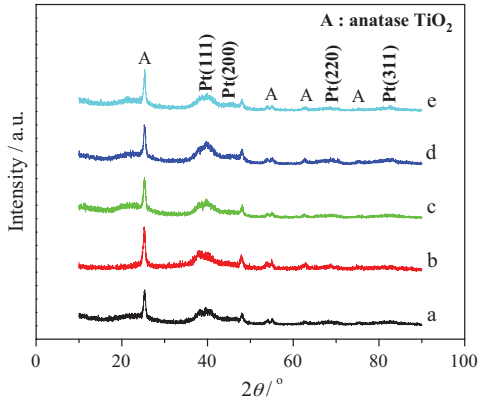

Fig. 1. XRD patterns of the Pt/TiO_2–C catalysts with various particle sizes of TiO_2: (a) 5 nm, (b) 20 nm, (c) 30 nm, (d) 50 nm, and (e) 70 nm.

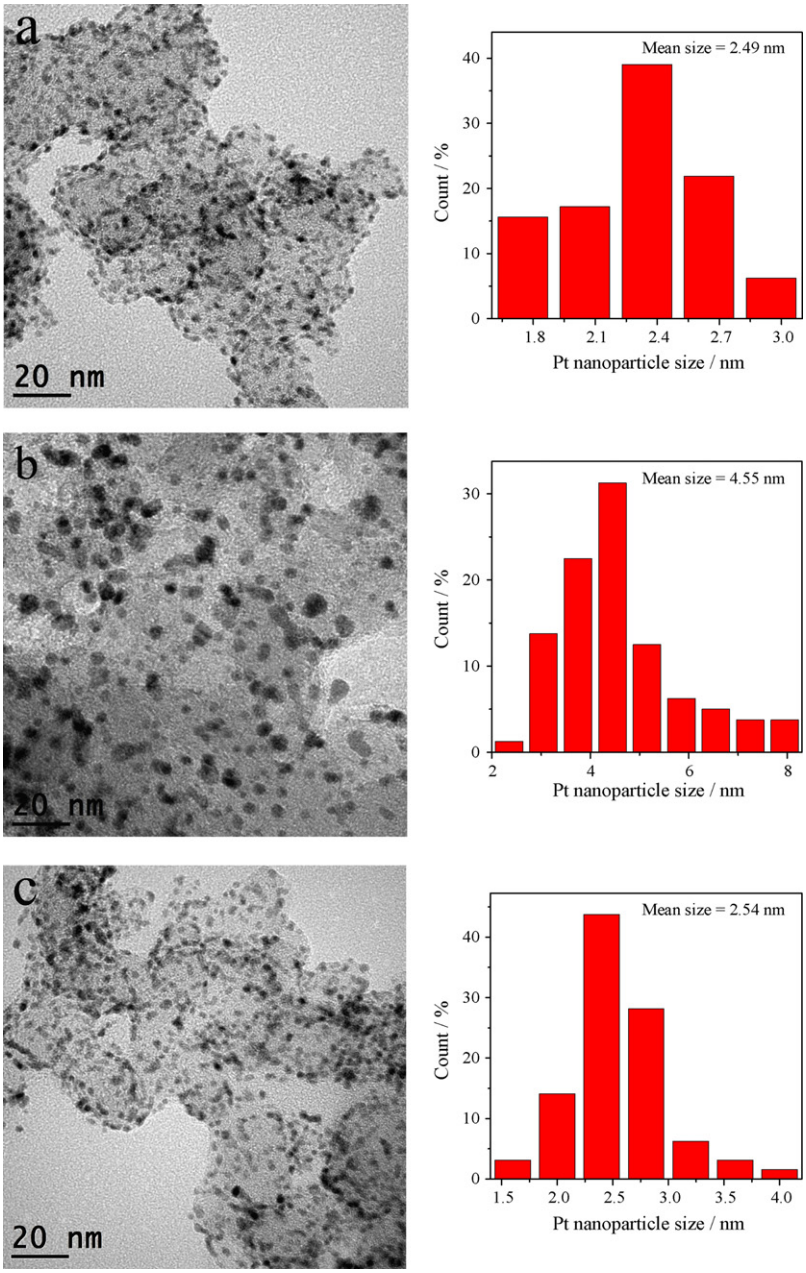

Fig. 2. TEM images and the size distributions of Pt/TiO_2–C catalysts with different particle sizes of TiO_2: (a, b) 5 nm, (c, d) 20 nm, (e, f) 70 nm before (a, c, e), and after (b, d, f) APCT.

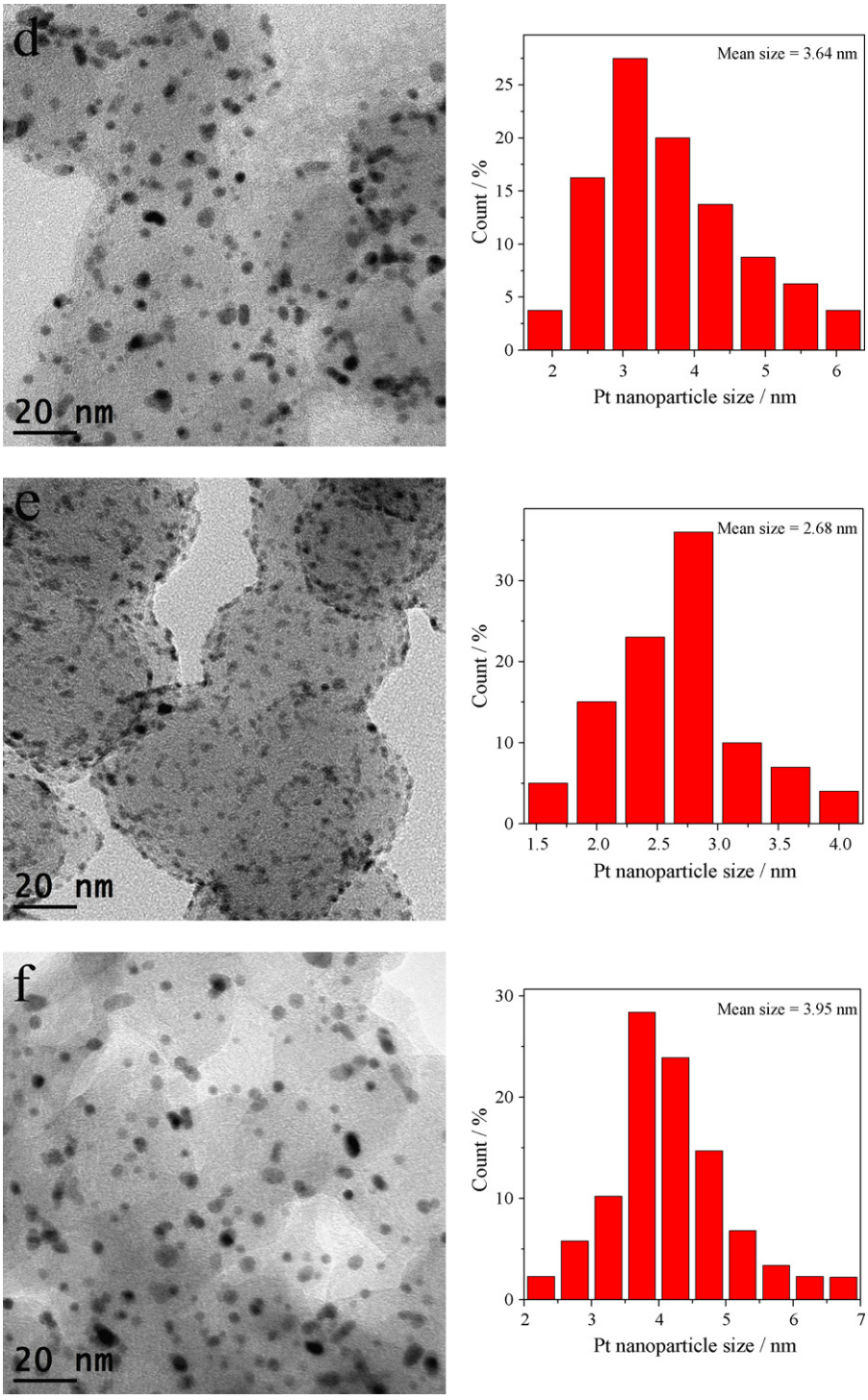

Fig. 2. (*Continued*).

at 20 wt.%. Briefly, a calculated amount of mixed support was dispersed into the mixture of ethylene glycol and isopropyl alcohol under ultrasonic treatment for 1 h. Then H_2PtCl_6-EG solution was added into the uniform carbon ink with urgent agitation for 3 h. The pH value of the ink was then adjusted to 12.0 and the suspension was subjected to consecutive microwave heating for 50 s. After cooling to room temperature, the pH value of the solution was adjusted to 3–4. The mixture was kept stirring for 12 h and then the product was washed repeatedly with ultrapure water (Millipore, 18.2 MΩ cm). The obtained Pt/TiO_2–C catalysts were dried for 3 h at 80 °C and then stored in a vacuum vessel.

2.2. Physical characterization

X-ray diffraction (XRD) measurements were carried out using the D/max-RB diffractometer with Cu K*a* radiation. The tube voltage was maintained at 45 kV and tube current at 100 mA. Diffraction patterns were collected with a scanning rate of 4° min^{-1} and with a step of 0.05°. The samples for transmission electron microscopy (TEM) analysis were prepared by ultrasonically dispersing the catalyst powder in ethanol. A drop of the suspension was then deposited and dried on a standard copper grid coated with carbon film. The morphology of the catalysts was characterized using a TECNAI G2

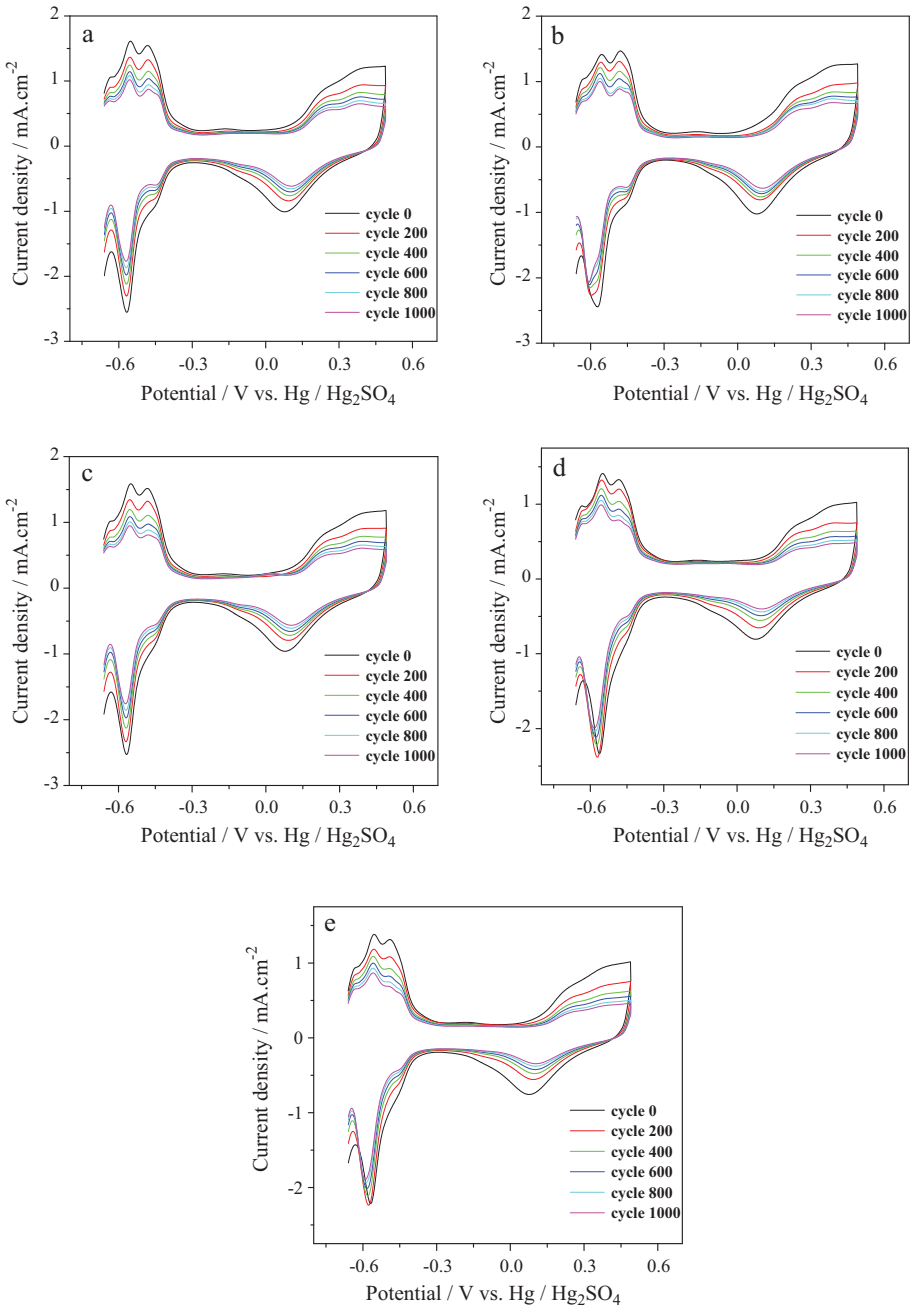

Fig. 3. Cyclic voltammograms in 0.5 mol L^{-1} H_2SO_4 for Pt/TiO_2–C with various particle sizes of TiO_2: (a) 5 nm, (b) 20 nm, (c) 30 nm, (d) 50 nm, and (e) 70 nm during the APCT. Scanning rate: 50 mV s^{-1}; test temperature: 25 °C.

F30 field emission transmission electron microscope operated at 300 kV.

2.3. Electrochemical characterization

Electrochemical measurements were performed using a CHI650D electrochemical analysis instrument and a conventional three-electrode cell. Porous electrodes were prepared as follows: 5.0 mg catalyst in 2.5 mL ethanol was ultrasonicated for 20 min. Then, 10 μL of this ink was transferred onto a glassy carbon disk (GC, 4 mm diameter), and onto which 5 μL of a dilute aqueous Nafion® solution (5 wt. % solution in a mixture of lower aliphatic alcohols and ultrapure water) was added. A piece of Pt foil (1 cm^2) was used as the counter electrode and the Hg/Hg_2SO_4 (−0.68 V relative to reversible hydrogen electrode, RHE) was used as the reference electrode. The cyclic voltammograms (CV) within a potential range from −0.66 V to 0.49 V were recorded to calculate the electrochemical active specific surface area (*ESA*) [18].

The investigation on the stability of Pt-based catalysts in PEMFCs is a time-consuming and complex task. To test the stability of catalysts in a real normally working PEMFC is inefficient because the life requirement for PEMFC is >5000 h for transportation and >40,000 h for stationary applications [19]. Therefore, the so-called accelerated degradation tests is developed. One of the accelerated degradation tests is potential cycling [20–22] which is carried out during the potential region between the oxidation and reduction of Pt. Herein, the accelerated potential cycling test (APCT) which was conducted within the potential range of −0.11–0.49 V (the region between the oxidation and reduction of Pt) was applied to evaluate the stability of catalysts. All experiments were carried out at a

temperature of 25 ± 1 °C and all the potentials reported here were referenced with respect to the Hg/Hg_2SO_4 electrode.

3. Results and discussion

3.1. Effects of anatase TiO_2 with different sizes on the stability of Pt catalysts

3.1.1. Physical characteristics of homemade various Pt/TiO_2–C catalysts

In this section, the mass fraction of TiO_2 in the mixed support is 40%. Fig. 1 shows the XRD patterns of Pt/TiO_2–C catalysts with various particle sizes of TiO_2. As a result of all kinds of TiO_2 used here is perfect anatase phase, it can be distinctly seen that all spectra of Pt/TiO_2–C catalysts are almost the same. Moreover, Pt diffraction peaks can be detected in all Pt/TiO_2–C patterns, however, not clear, which is similar to our previous work [18]. For the sake of convenience and concision, Pt/TiO_2–C with TiO_2 particle sizes of 5 nm, 20 nm, 30 nm, 50 nm, and 70 nm are denoted as Pt/TiO_2–C-5, Pt/TiO_2–C-20, Pt/TiO_2–C-30, Pt/TiO_2–C-50, and Pt/TiO_2–C-70, respectively.

TEM images with associated size distributions of Pt/TiO_2–C-5, Pt/TiO_2–C-20, and Pt/TiO_2–C-70 before and after APCT are shown in Fig. 2. The TEM micrographs illustrate clearly that the dispersion of Pt nanoparticles on the mixed supports before APCT is fairly uniform. Pt particle sizes slightly increase with the increasing of particle sizes of TiO_2. Fig. 2a and c shows that the mean size of Pt nanoparticles of Pt/TiO_2–C-5 is similar to that of Pt/TiO_2–C-20, indicating that Pt/TiO_2–C-5 and Pt/TiO_2–C-20 has almost the same activity. However, the mean size of Pt nanoparticles of Pt/TiO_2–C-70 is evidently larger than Pt/TiO_2–C-5 and Pt/TiO_2–C-20, showing that the activity of Pt/TiO_2–C-70 is lower than those of Pt/TiO_2–C-5 and Pt/TiO_2–C-20 catalysts. As to the TEM micrographs after APCT, it can be obviously seen that the crystallite sizes of Pt/TiO_2–C-5, Pt/TiO_2–C-20, and Pt/TiO_2–C-70 grow to 4.55 nm, 3.64 nm, and 3.95 nm, increasing by 82.7%, 43.3%, and 47.4% in comparison with those before APCT, respectively. The results after APCT indicate that Pt/TiO_2–C-20 has higher stability than Pt/TiO_2–C-5 and Pt/TiO_2–C-70 catalysts.

3.1.2. Electrochemical characteristics of homemade various Pt/TiO_2–C catalysts

APCT of Pt/TiO_2–C-5, Pt/TiO_2–C-20, Pt/TiO_2–C-30, Pt/TiO_2–C-50, and Pt/TiO_2–C-70 are carried out in 0.5 mol L^{-1} H_2SO_4 at 25 °C. Cyclic voltammograms (CV) before and after APCT are shown in Fig. 3. Measurements of the hydrogen adsorption–desorption (HAD) integrals provide the *ESA* of Pt nanoparticles. The *ESA* and relative *ESA* of various Pt/TiO_2–C catalysts with cycle number during the APCT are shown in Figs. 4 and 5, respectively. As shown in Fig. 4, the original *ESA* of the catalyst decreases with the increase of mean particle size of TiO_2, which is in accordance with the results of TEM. However, it can be clearly seen that the activity of the Pt/TiO_2–C-20 is almost the same with that of Pt/TiO_2–C-5 and the stability of the Pt/TiO_2–C-20 catalyst is the best after 1000 cycles APCT, illustrating that the optimized particle size of TiO_2 in the Pt/TiO_2–C catalyst is 20 nm.

3.2. Effects of anatase TiO_2 with different contents on the stability of Pt catalysts

3.2.1. Physical characteristics of homemade various Pt/TiO_2–C catalysts

The mean particle size of TiO_2 used in this part is 20 nm. XRD patterns of Pt/TiO_2–C with different contents of TiO_2 are presented in Fig. 6. The spectra of various Pt/TiO_2–C catalysts are very similar to the results of Fig. 1. In this section, the expression of TiO_2 contents

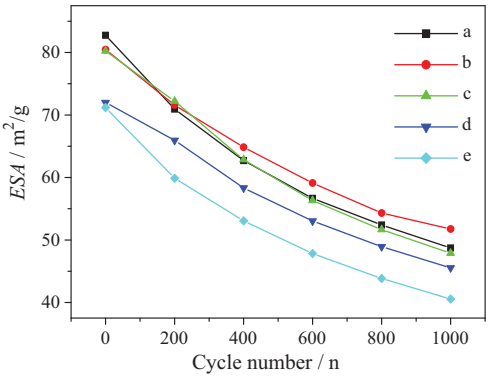

Fig. 4. *ESA* of Pt/TiO_2–C with various particle sizes of TiO_2: (a) 5 nm, (b) 20 nm, (c) 30 nm, (d) 50 nm, and (e) 70 nm.

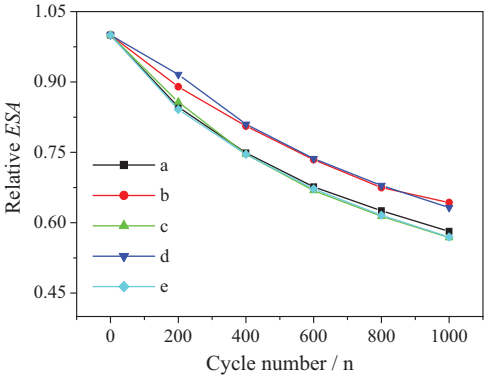

Fig. 5. Relationship of *ESA* and cycle numbers of Pt/TiO_2–C with various particle sizes of TiO_2: (a) 5 nm, (b) 20 nm, (c) 30 nm, (d) 50 nm, and (e) 70 nm during the APCT.

in the catalysts is relative to the total mass of mixed support. The equation is presented as follows:

$$TiO_2\% = \frac{TiO_2 \text{ mass}}{TiO_2 \text{ mass} + \text{carbon black mass}} \quad (1)$$

For the sake of convenience in the expression, Pt/TiO_2–C with 30%, 40%, 50%, 60%, 70%, 80% and 90% TiO_2 are designated as Pt/TiO_2–C-30%, Pt/TiO_2–C-40%, Pt/TiO_2–C-50%, Pt/TiO_2–C-60%, Pt/TiO_2–C-70%, Pt/TiO_2–C-80%, and Pt/TiO_2–C-90%, respectively.

Fig. 7 shows TEM images with associated size distributions of Pt/TiO_2–C-70%, Pt/TiO_2–C-50%, and Pt/TiO_2–C-30% before and after APCT, respectively. The TEM micrographs illustrate clearly that

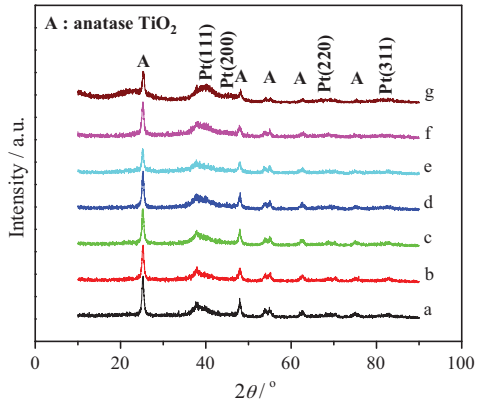

Fig. 6. XRD patterns of Pt/TiO_2–C catalysts with different contents of TiO_2: (a) 90%, (b) 80%, (c) 70%, (d) 60%, (e) 50%, (f) 40%, and (g) 30%.

the dispersion of Pt nanoparticles on the mixed supports before APCT is fairly uniform. According to the expression, the experimental results of Pt/TiO_2–C-40% are the same with Pt/TiO_2–C-20 mentioned above. From Figs. 7(a) (c) and (e) and 2(c), it can be clearly seen that the mean sizes of Pt nanoparticles are almost the same before APCT. However, after APCT, the crystallite sizes of Pt/TiO_2–C-70%, Pt/TiO_2–C-50%, Pt/TiO_2–C-40% (Pt/TiO_2–C-20), and Pt/TiO_2–C-30% increased by 0.98 nm, 1.10 nm, 1.10 nm, and 1.34 nm in comparison with those before APCT, respectively, showing that the stability of the catalyst increases with the increase of the content of TiO_2. The reason is that there is strong metal–support interaction (SMSI) [18,23,24], which becomes stronger with the increase of TiO_2 content in the mixed supports, between Pt nanoparticles and TiO_2. SMSI between Pt and TiO_2 [23–27] has been studied and confirmed by many investigators. Pt supported on TiO_2 or composite support has also been used in the field of fuel cells. Huang and his co-workers [28] thought the ultrahigh stability of the Pt/TiO_2 catalyst was attributed to the SMSI between Pt particles and TiO_2 support for PEMFCs. In our previous work, carbon riveted Pt/TiO_2–C [18] and carbon riveted microcapsule Pt/MWCNTs-TiO_2 [29] have also been synthesized. The experimental results indicate that carbon riveted Pt/TiO_2–C and carbon riveted microcapsule

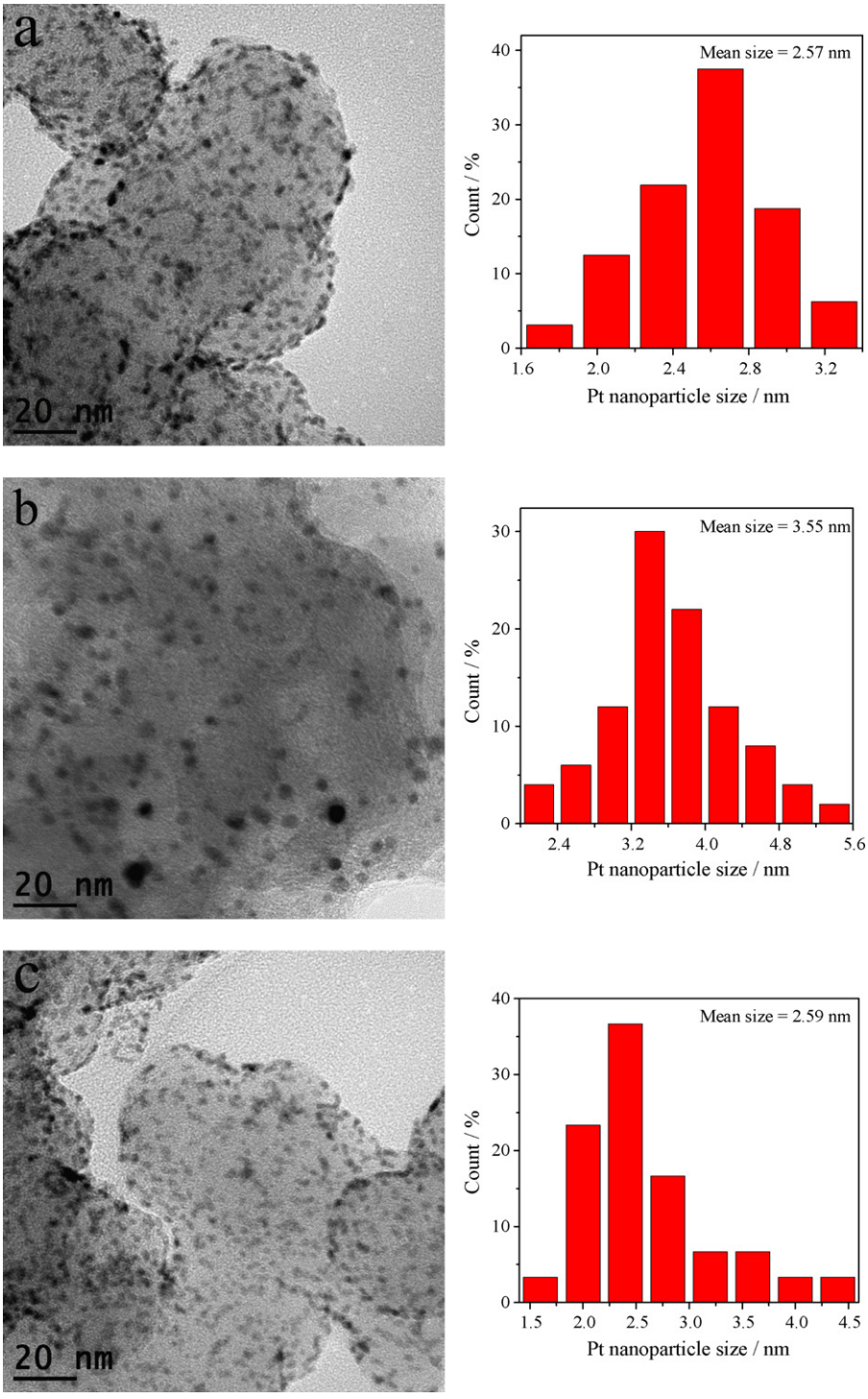

Fig. 7. TEM images and the size distributions of Pt/TiO_2–C catalysts with different contents of TiO_2: (a, b) 70%, (c, d) 50%, (e, f) 30% before (a, c, e), and after (b, d, f) APCT.

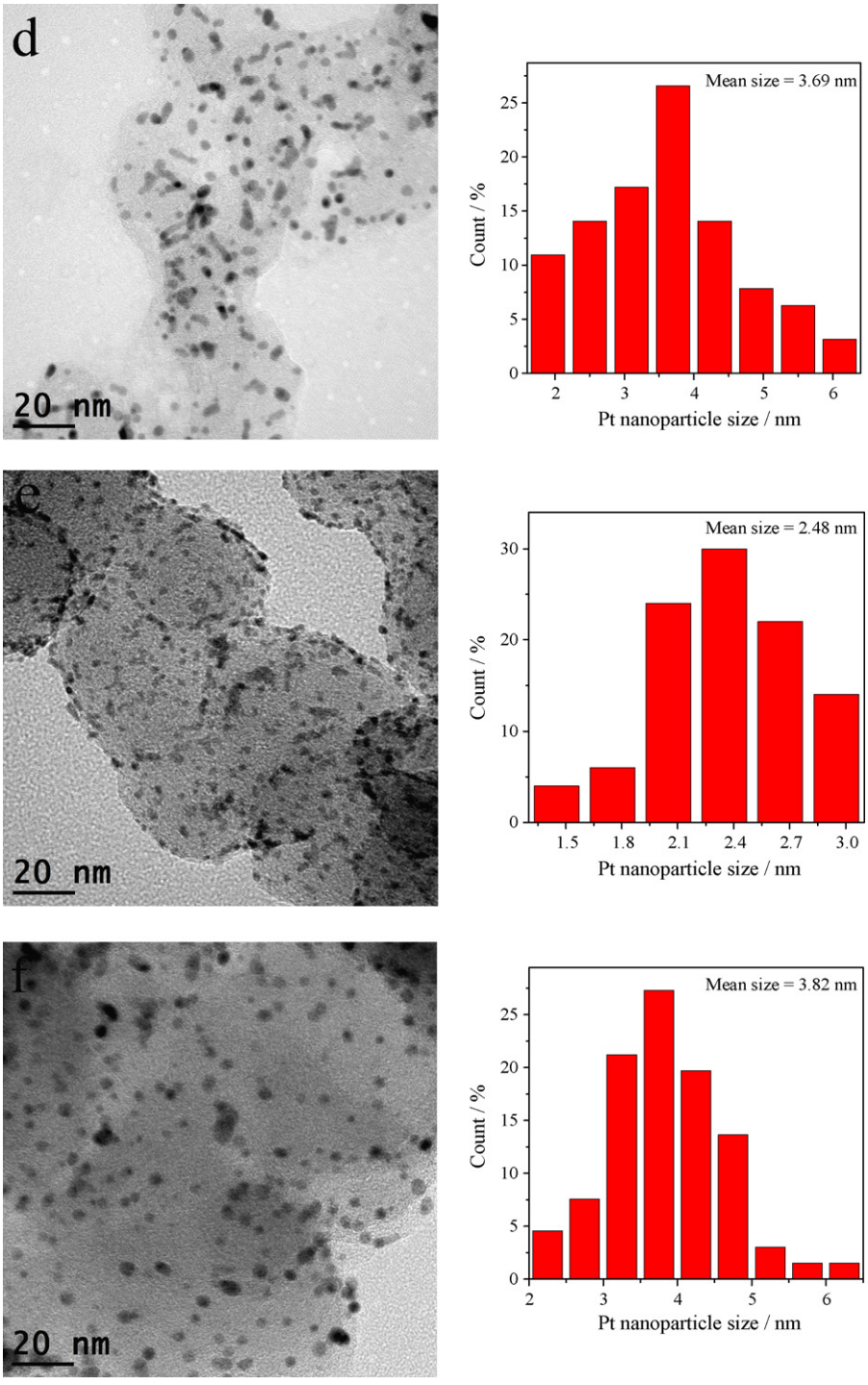

Fig. 7. (*Continued*)

Pt/MWCNTs-TiO_2 exhibit both high activity and stability due to SMSI between Pt nanoparticles and TiO_2. TiO_2 may anchor the Pt particles by interacting with Pt and thereby inhibit Pt migration and agglomeration and then improve the stability of Pt-based catalyst [30].

3.2.2. *Electrochemical characteristics of homemade various Pt/TiO_2–C catalysts*

APCT of Pt/TiO_2–C-90%, Pt/TiO_2–C-80%, Pt/TiO_2–C-70%, Pt/TiO_2–C-60%, Pt/TiO_2–C-50%, Pt/TiO_2–C-40%, and Pt/TiO_2–C-30% are carried out in 0.5 mol L^{-1} H_2SO_4 at 25 °C. Cyclic voltammograms (CV) before and after APCT are shown in Fig. 8. The *ESA* and relative *ESA* of various Pt/TiO_2–C catalysts with cycle number during the APCT are shown in Figs. 9 and 10, respectively. According to the results of Fig. 7, the mean sizes of Pt nanoparticles before APCT are almost the same. However, as shown in Fig. 9, the original *ESA* of the catalyst decreases drastically with the increasing of TiO_2 content which is due to the poor conductivity of TiO_2. That is, the more TiO_2 content exists in the catalyst, the worse conductivity of the mixed support exhibits, and then the worse activity of the catalyst is presented. Furthermore, it can also be distinctly observed that the stability of the catalyst increases with the increase of TiO_2 content, which is in accordance with the TEM results of Fig. 7. In addition, when TiO_2 content in the mixed

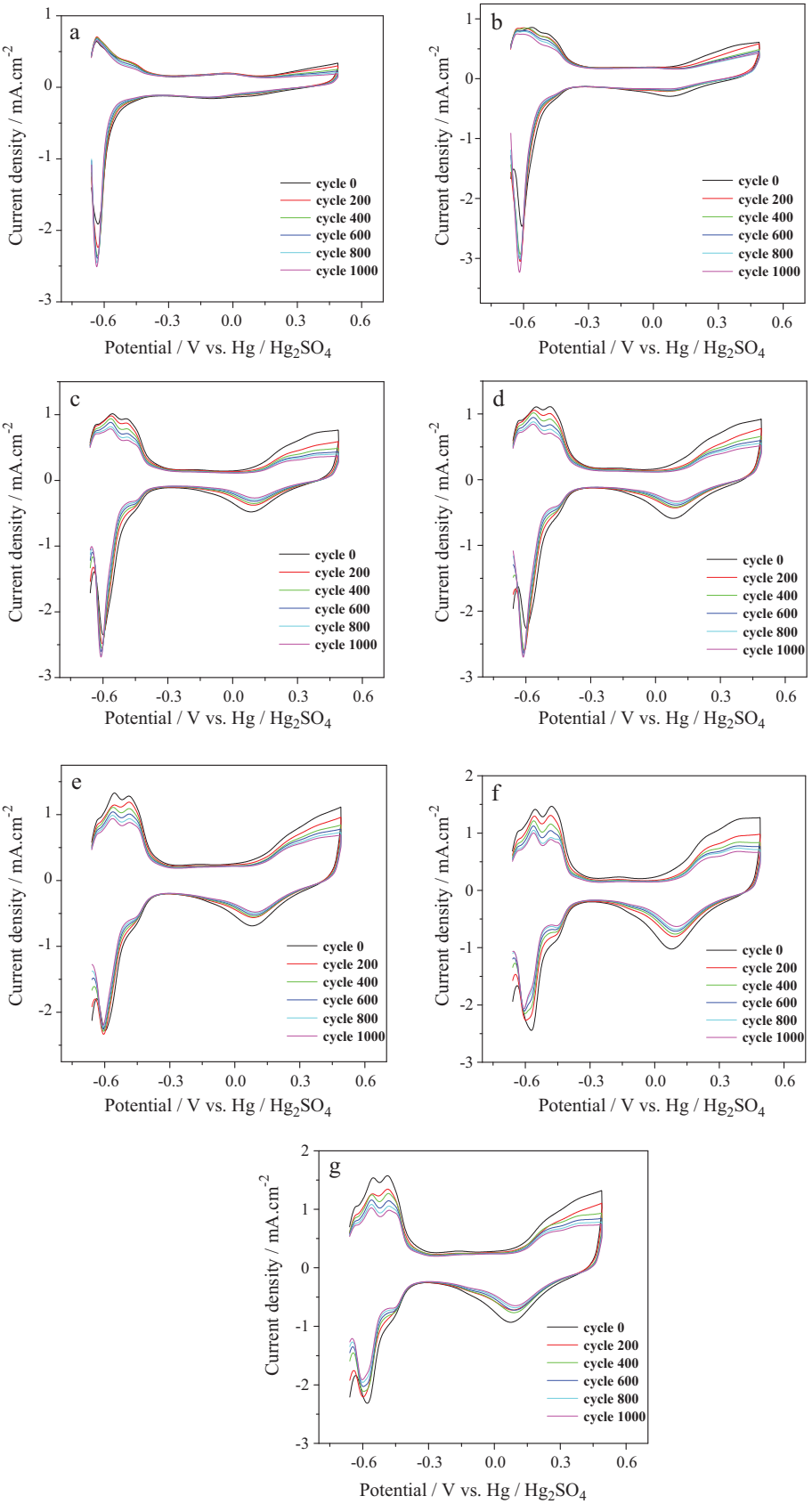

Fig. 8. Cyclic voltammograms in 0.5 mol L^{-1} H_2SO_4 for Pt/TiO_2–C catalysts with different contents of TiO_2: (a) 90%, (b) 80%, (c) 70%, (d) 60%, (e) 50%, (f) 40%, and (g) 30% during the APCT. Scanning rate: 50 mV s^{-1}; test temperature: 25 °C.

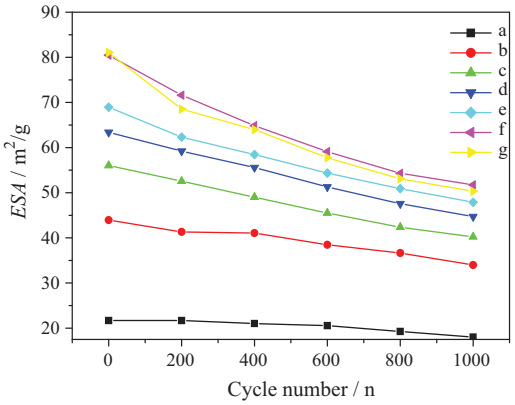

Fig. 9. *ESA* of Pt/TiO_2–C with different content of TiO_2: (a) 90%, (b) 80%, (c) 70%, (d) 60%, (e) 50%, (f) 40%, and (g) 30%.

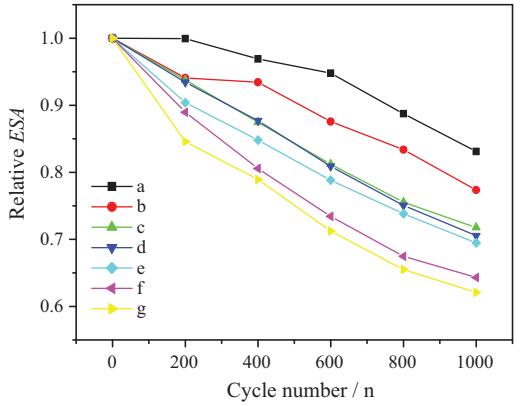

Fig. 10. Relationship of *ESA* and cycle numbers of Pt/TiO_2–C catalysts with different contents of TiO_2: (a) 90%, (b) 80%, (c) 70%, (d) 60%, (e) 50%, (f) 40%, and (g) 30% during the APCT.

support is 40%, the obtained Pt/TiO_2–C catalyst with almost the same activity compared with the Pt/C Exhibits 14% higher stability than Pt/C after 1000 cycles APCT [18]. From both the activity and stability of the various Pt/TiO_2–C catalysts, 40% TiO_2 existed in the mixed support is the optimized TiO_2 content in this work.

4. Conclusions

Pt/TiO_2–C catalysts with different particle sizes and contents of TiO_2 have been synthesized by microwave-assisted polyol process (MAPP). Some physical and electrochemical techniques have been carried out to present the influence degree of different particle sizes and contents of TiO_2. The experimental results indicate that the original *ESA* of the catalyst decreases with the increase of mean particle size of TiO_2 and TiO_2 content. The stability of the catalyst increases with the increase of TiO_2 content in the mixed support due to the increase of SMSI between Pt and TiO_2. Taking into account both the activity and stability of the various Pt/TiO_2–C catalysts, the optimized particle size of TiO_2 is 20 nm and 40% TiO_2 existed in the mixed support is optimal. Full tests of these supported catalysts in single fuel cells are still in process. Considering the importance of the stability of the catalysts in fuel cell environments and the rapidness, simplicity, uniformity as well as efficiency of synthesis procedure of the catalysts, the Pt/TiO_2–C is a promising catalyst for PEMFCs.

Acknowledgments

This research is financially supported by the National Natural Science Foundation of China (Grant No. 20606007), the Scientific Research Foundation for the Returned Overseas Chinese Scholars, State Education Ministry (2008), and Scientific Research Foundation for Returned Scholars of Heilongjiang Province of China (LC08C33).

References

[1] Z.-Z. Jiang, Z.-B. Wang, D.-M. Gu, E.S. Smotkin, Chem. Commun. 46 (2010) 6998–7000.
[2] Z.B. Wang, C.R. Zhao, P.F. Shi, Y.S. Yang, Z.B. Yu, W.K. Wang, G.P. Yin, J. Phys. Chem. C 114 (2010) 672–677.
[3] C. Koenigsmann, S.S. Wong, Energ. Environ. Sci. 4 (2011) 1161–1176.
[4] G.J.K. Acres, J. Power Sources 100 (2001) 60–66.
[5] Z.-B. Wang, G.-P. Yin, Y.-G. Lin, J. Power Sources 170 (2007) 242–250.
[6] S.C. Zignani, E. Antolini, E.R. Gonzalez, J. Power Sources 182 (2008) 83–90.
[7] E. Lebègue, S. Baranton, C. Coutanceau, J. Power Sources 196 (2011) 920–927.
[8] L.M. Roen, C.H. Paik, T.D. Jarvi, Electrochem. Solid-State Lett. 7 (2004) A19–A22.
[9] J.J. Wang, G.P. Yin, Y.Y. Shao, S. Zhang, Z.B. Wang, Y.Z. Gao, J. Power Sources 171 (2007) 331–339.
[10] Z.-B. Wang, P.-J. Zuo, X.-P. Wang, J. Lou, B.-Q. Yang, G.-P. Yin, J. Power Sources 184 (2008) 245–250.
[11] W. Li, A.M. Lane, Electrochim. Acta 55 (2010) 6926–6931.
[12] R. Borup, J. Meyers, B. Pivovar, Y.S. Kim, R. Mukundan, N. Garland, D. Myers, M. Wilson, F. Garzon, D. Wood, P. Zelenay, K. More, K. Stroh, T. Zawodzinski, J. Boncella, J.E. McGrath, M. Inaba, K. Miyatake, M. Hori, K. Ota, Z. Ogumi, S. Miyata, A. Nishikata, Z. Siroma, Y. Uchimoto, K. Yasuda, K.I. Kimijima, N. Iwashita, Chem. Rev. 107 (2007) 3904–3951.
[13] J. Shim, C.-R. Lee, H.-K. Lee, J.-S. Lee, E.J. Cairns, J. Power Sources 102 (2001) 172–177.
[14] S. von Kraemer, K. Wikander, G. Lindbergh, A. Lundblad, A.E.C. Palmqvist, J. Power Sources 180 (2008) 185–190.
[15] S.L. Gojkovic, B.M. Babic, V.R. Radmilovic, N.V. Krstajic, J. Electroanal. Chem. 639 (2010) 161–166.
[16] L. Xiong, A. Manthiram, Electrochim. Acta 49 (2004) 4163–4170.
[17] X. Liu, J. Chen, G. Liu, L. Zhang, H. Zhang, B. Yi, J. Power Sources 195 (2010) 4098–4103.
[18] Z.-Z. Jiang, Z.-B. Wang, Y.-Y. Chu, D.-M. Gu, G.-P. Yin, Energ. Environ. Sci. 4 (2011) 728–735.
[19] Y.Y. Shao, G.P. Yin, Y.Z. Gao, J. Power Sources 171 (2007) 558–566.
[20] G. Gupta, D.A. Slanac, P. Kumar, J.D. Wiggins-Camacho, X.Q. Wang, S. Swinnea, K.L. More, S. Dai, K.J. Stevenson, K.P. Johnston, Chem. Mater. 21 (2009) 4515–4526.
[21] J. Zhang, K. Sasaki, E. Sutter, R.R. Adzic, Science 315 (2007) 220–222.
[22] S. Mitsushima, S. Kawahara, K.-i. Ota, N. Kamiya, J. Electrochem. Soc. 154 (2007) B153–B158.
[23] S.J. Tauster, S.C. Fung, R.T.K. Baker, J.A. Horsley, Science 211 (1981) 1121–1125.
[24] J.M. Herrmann, M. Gravelle-Rumeau-Maillot, P.C. Gravelle, J. Catal. 104 (1987) 136–146.
[25] R.T.K. Baker, E.B. Prestridge, R.L. Garten, J. Catal. 59 (1979) 293–302.
[26] A. Dauscher, L. Hilaire, F. Le Normand, W. Müller, G. Maire, A. Vasquez, Surf. Interface Anal. 16 (1990) 341–346.
[27] O. Dulub, W. Hebenstreit, U. Diebold, Phys. Rev. Lett. 84 (2000) 3646.
[28] S.-Y. Huang, P. Ganesan, S. Park, B.N. Popov, J. Am. Chem. Soc. 131 (2009) 13898–13899.
[29] Z.-Z. Jiang, Z.-B. Wang, Y.-Y. Chu, D.-M. Gu, G.-P. Yin, Energ. Environ. Sci. (2011), 10.1039/C1EE01091C.
[30] C.-C. Shih, J.-R. Chang, J. Catal. 240 (2006) 137–150.